Presented at Second Joint US Army SDC/BNL Neutralizer Workshop, June 17-18, 1986

BNL--39022

DE87 005249

MEASUREMENT OF PLASMA PRODUCTION AND NEUTRALIZATION IN GAS NEUTRALIZERS *

D. Maor, M. Meron, B. Johnson, K. Jones, A. Agagu and B. Hu
Brookhaven National Laboratory
Upton, N.Y. 11973

Several previous talks have emphasized the need of experimental data for the designing of gas neutralizers. We have started a project aimed at measuring all relevant cross sections for the charge exchange of H^-, H^0 and H^+ projectiles, as well as the cross sections for the production of ions in the target. The expected results of these latter measurements are shown schematically in Transparency No. 1. Each square in the table represents a full charge state distribution of recoiling ions in coincidence with the colliding hydrogen ion of given incoming and given outgoing charge state. The diagonal elements represent cross sections for production of recoiling ions with different charge states in collisions where the projectile does not undergo a charge exchange.

The results of these experiments will give important information on the following questions:

1. Absolute values and energy dependence of stripping cross sections for H^- and H^0 are sorely needed for the accurate design of the gas neutralizer.

2. The total charge produced in the target and its distribution is a critical input for the calculation of the plasma density and the determination of its effect on beam divergence (see preceding paper by A. Sonin and C.C. Lin).

3. Since the experiments will be performed on many gases, differences in both neutralization efficiency and plasma production can be determined, providing an important input to the final choice of the neutralizer gas.

4. The cross sections for ion production without projectile charge exchange for H^- and H^0 will give indirect but important information on the contribution of such collisions to beam divergence, a factor which, due to lack of information, has been disregarded in theoretical calculations.

*This work was performed under the sponsorship of the United States Army SDC, contract No. MIPR W31RPD-63-A169 and the Fundamental Interactions Branch, Division of Chemical Sciences, Office of Basic Energy Sciences, US Department of Energy, Contract DE-AC02-76CH00016.

The experiments will make use of two unique BNL facilities. The first stage of experiments will be performed at the MP6 Tandem Van de Graaff accelerator. This accelerator is equipped with a source at the high energy terminal and can be run at negative voltage. As a result, negative ions (including H^-) can be produced and accelerated to energies of 2-10 MeV. In the next stage, the experiments will be performed at the 200 MeV BNL Linac.

The location of the H^- source and the beam path are shown in Transparency No. 2 which is a schematic of the BNL double-Tandem facility. Transparency No. 3 shows a schematic of the experimental beam line. Gas cell 1 is for the production of positive ions or the reduction of the H^- beam intensity, gas cell 2, in conjecture with the first deflector, results in the production of a neutral beam. The position of the first deflector and the anti-scatter collimator have been interchanged in the actual experiment. Also, the first deflector deflects in the horizontal plane while the second one deflects in the vertical plane.

Transparency No. 4 shows in more detail the target area, including the recoil time-of-flight (RTOF) spectrometer. The electrons and ions produced in the gas are extracted by two grids, designated + and −. The electrons impinge directly on a microchannel plate detector (MCP), while the ions first pass through a specially designed drift space. Thus, the time of arrival at the MCP uniquely determines their charge state. The recoiling ions are detected in coincidence with the electrons and the different charge states of the emerging projectiles.

Transparencies Nos. 5 and 6 are photographs of the beam line during a preliminary run. Transparency No. 7 is a photograph of a phosphor screen situated in the beam path (the viewer in transparencies 5 and 6). Operating both the pre- and post-deflectors and choosing an appropriate pressure in the neutralizer gas cell, all three components H^+, H° and H^- could be obtained in comparable intensities and separated both horizontally and vertically.

Transparencies Nos. 8 and 9 display the available experimental cross sections for the one-electron and two-electron stripping of H^-. The circles represent our preliminary results at 2.5, 5.6 and 8.0 MeV. The two additional data points for N_2 and Ar target gases are from two different sources in the literature, one at 10 MeV and the other at 14.6 MeV. Although there seems to be some systematic problem in our preliminary data, the data points seem to follow the 1/E dependence predicted by the Born approximation for stripping cross sections in this energy region, as shown in the transparencies for the N_2 target.

Transparency No. 10 displays the stripping cross section of the H° projectile. Here some more data points are available in the literature for N_2 and Ar targets. The circles represent our preliminary results. Again it can be seen that the N_2 data points seem to follow the 1/E line, to the available accuracy. However, surprisingly, the Ar data would be in much better agreement with a $1/E^{0.8}$ line. Considering the quality of the available data, this may be a spurious occurrence, but clearly more measurements are needed.

Transparency No.11 displays the neutralization efficiency as a function of projectile energy. The neutralization efficiency is defined as the maximum neutral fraction obtainable, using a target of optimum thickness, and is calculated from the previous cross section. The data points represent our results (circles) and other results for N_2 and Ar, and the dotted line represents data from literature for H_2 target gas. The dependence of the efficiency on both target gas and projectile energy is very weak. Still, the efficiency seems to decrease slightly with the increasing atomic number of the target gas. Since the use of very light targets, such as H_2, does not appear to be practical we have decided to include in our future studies gases with relatively large molecules of low-Z atoms, such as hydrocarbons. Also, when trying to extrapolate to a projectile energy of 200 MeV, one would tend to draw a slightly declining curve, arriving at an efficiency value of about 45%, which is considerably lower than the presently accepted 57%. Again, this might be just an artifact due to the scarcity of available data and further measurements are necessary.

After performing the proposed experiments on the Tandem Van de Graaff accelerator, the following steps are planned:

1. Linac Experiment. The whole apparatus for the detection of the recoils can be transferred without changes from the Tandem to the 200 MeV BNL Linac. The charge separation and detection of the projectiles at the Linac are also feasible. Thus, since the experiment can be performed at several energies, interpolation and extrapolation to any relevant energy is possible.

2. Ejected electron spectroscopy. The average kineic energy of the ejected electrons and their distribution is the crucial factor in determining the expected charge imbalance in the target plasma (see preceding paper by A. Sonin and C.C. Lin). The electron spectrum can readily be measured in both the Tandem and Linac experiments by adding an electron spectrometer to the available setup.

3. Charge production in thick targets. All previous measurements are to be performed on thin gas targets in order to measure accurate cross sections. However, additional target ions can be produced in thick targets by the electrons ejected in primary collisions. Also, the energy distribution of the electrons will change in a thick target due to their frequent collisions. It is thus proposed to develop a thick gas target, where these effects can be measured.

out \ in	-1	0	1
-1	$\sigma_{-1,-1}(q_T)$	$\sigma_{0,-1}(q_T)$	$\sigma_{1,-1}(q_T)$
0	$\sigma_{-1,0}(q_T)$	$\sigma_{0,0}(q_T)$	$\sigma_{1,0}(q_T)$
1	$\sigma_{-1,1}(q_T)$	$\sigma_{0,1}(q_T)$	$\sigma_{1,1}(q_T)$

9 Recoil charge state distributions

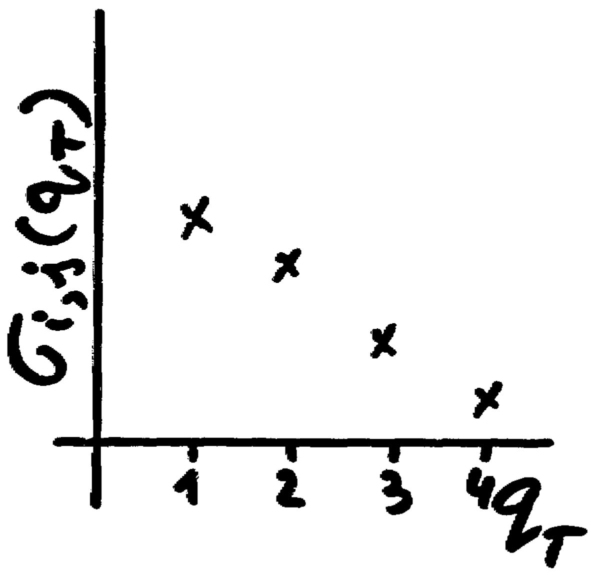

TRANSPARENCY NO. 2

TANDEM VAN DE GRAAFF FACILITY
BROOKHAVEN NATIONAL LABORATORY

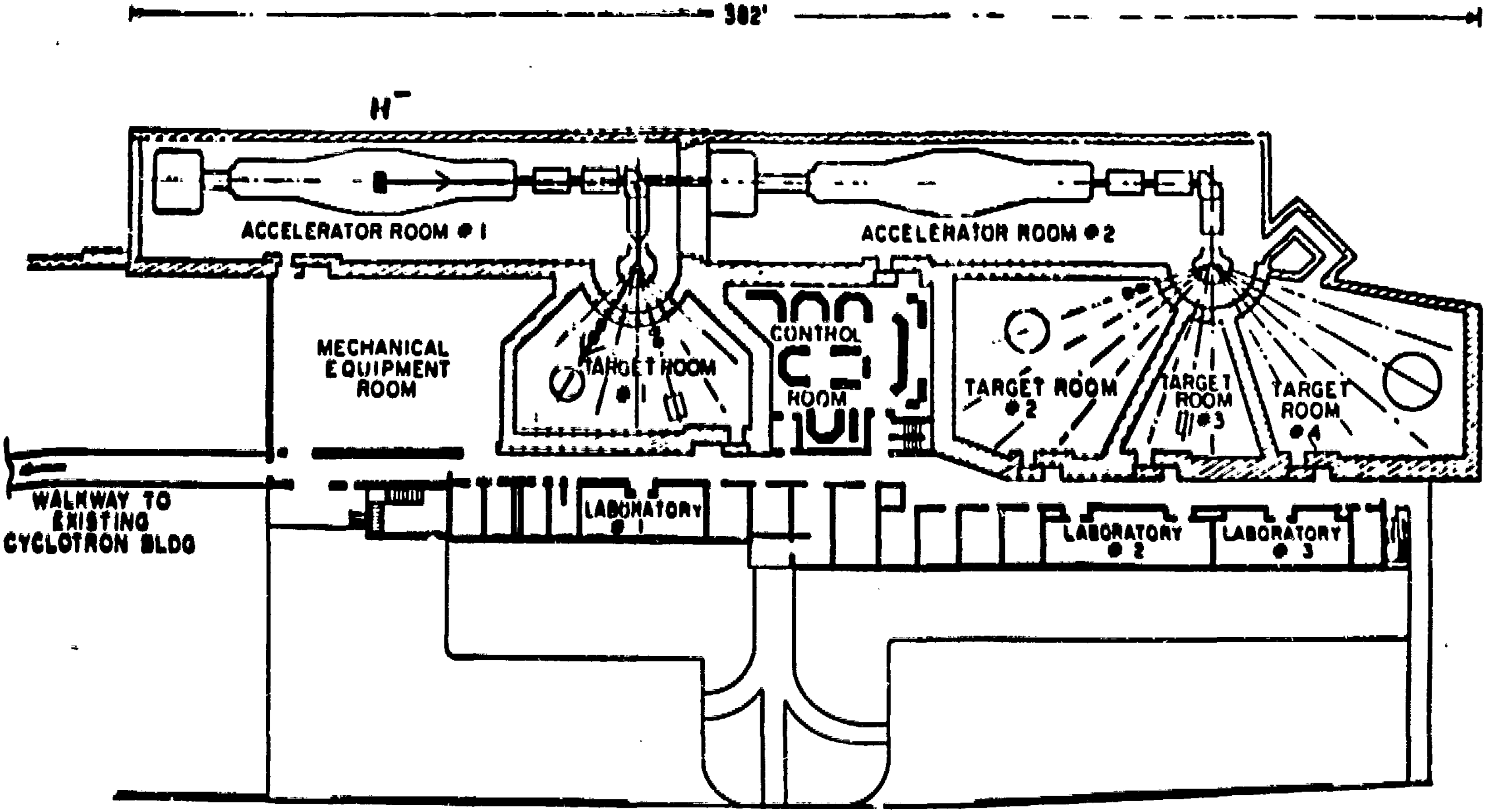

FIRST FLOOR PLAN

TRANSPARENCY NO. 3

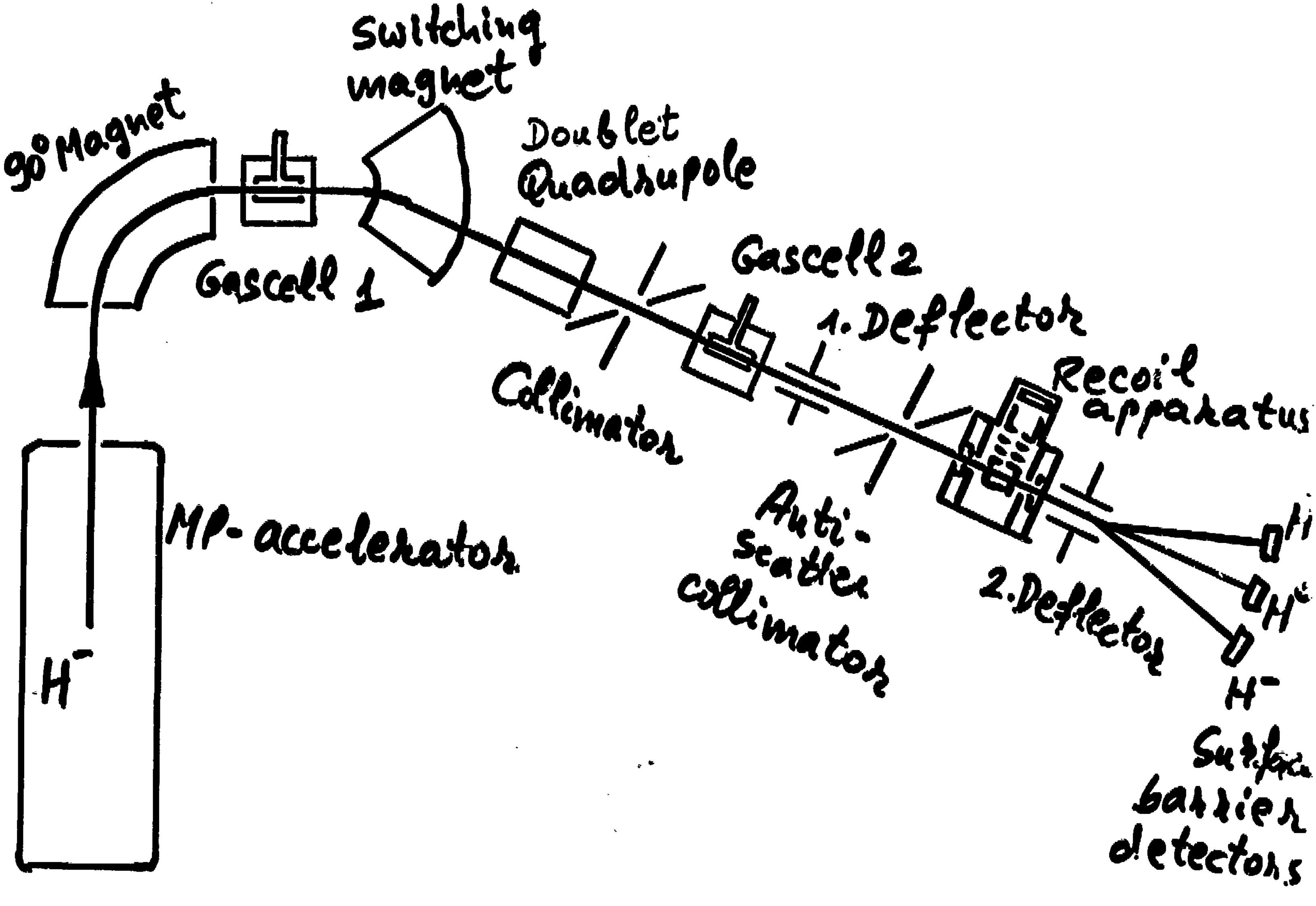

TRANSPARENCY NO. 4

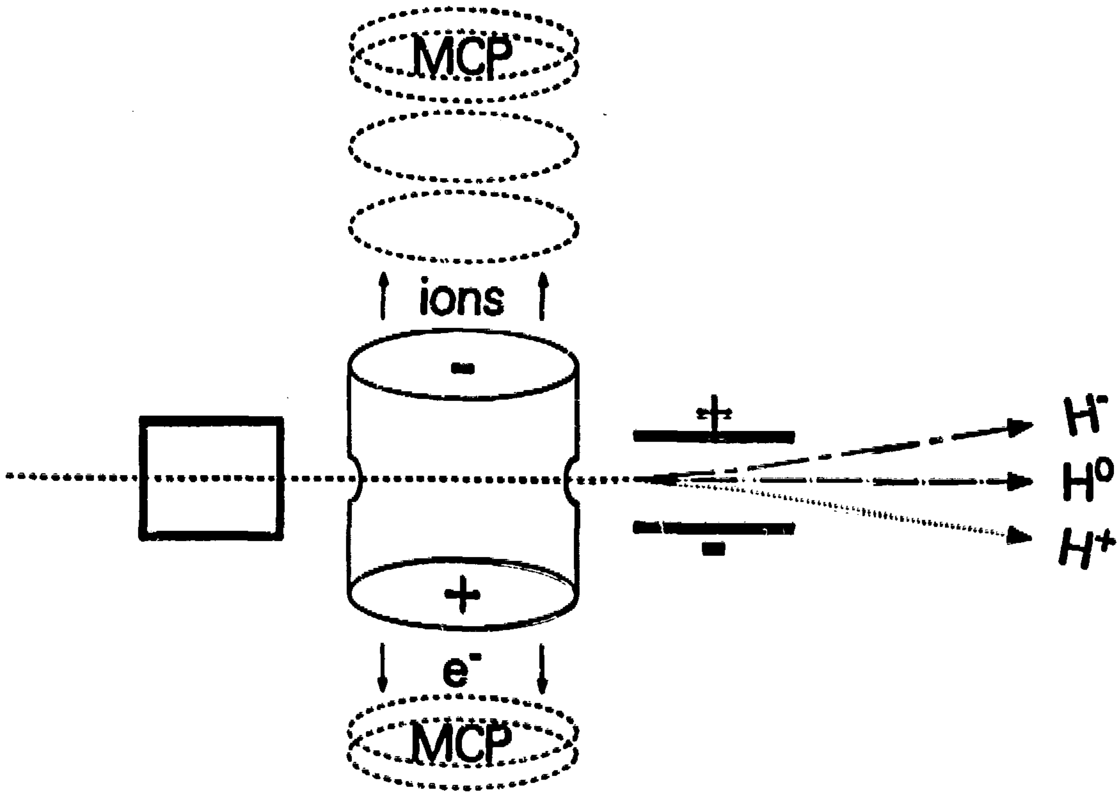

TRANSPARENCY NO. 5

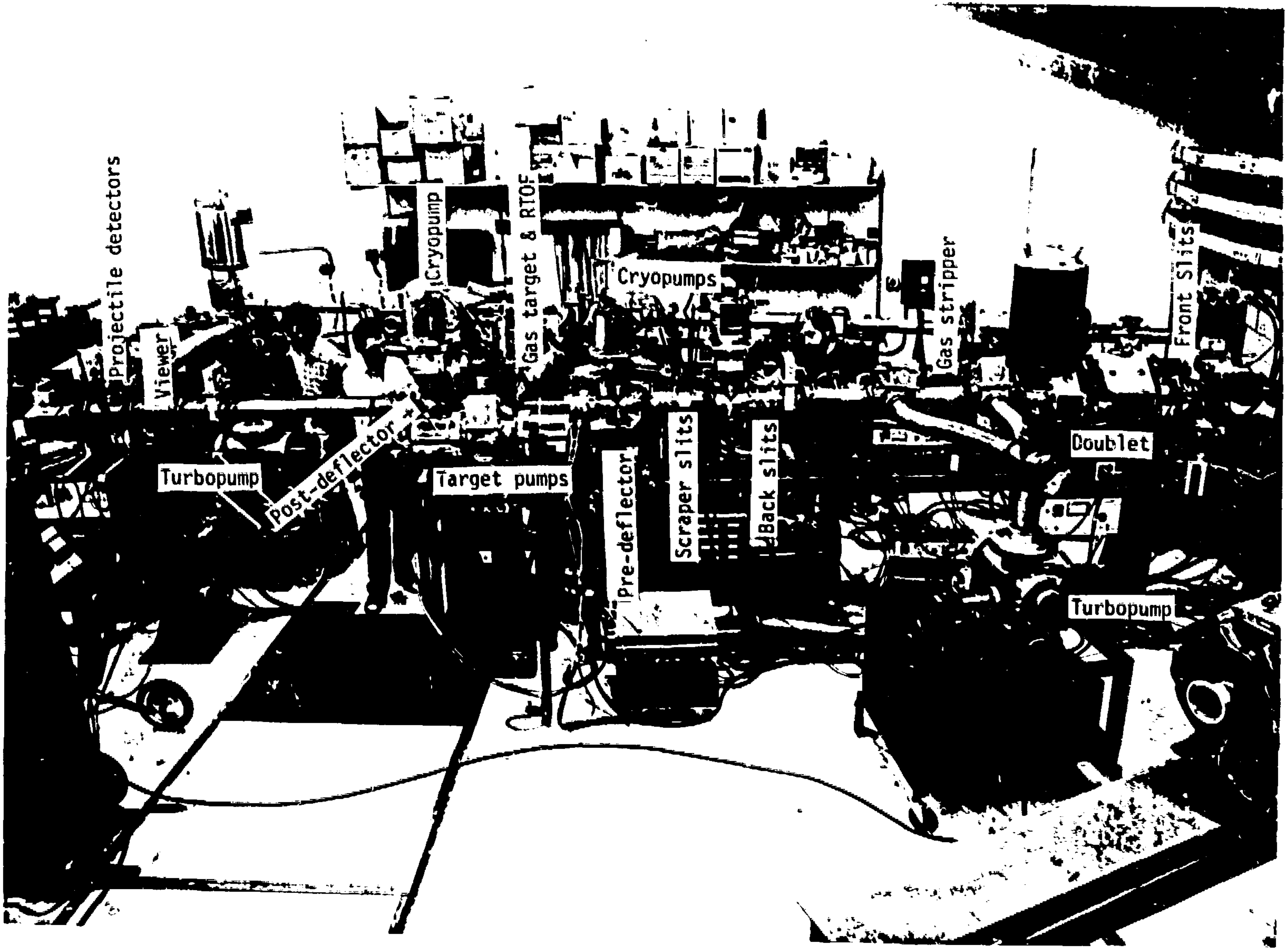

TRANSPARENCY NO. 6

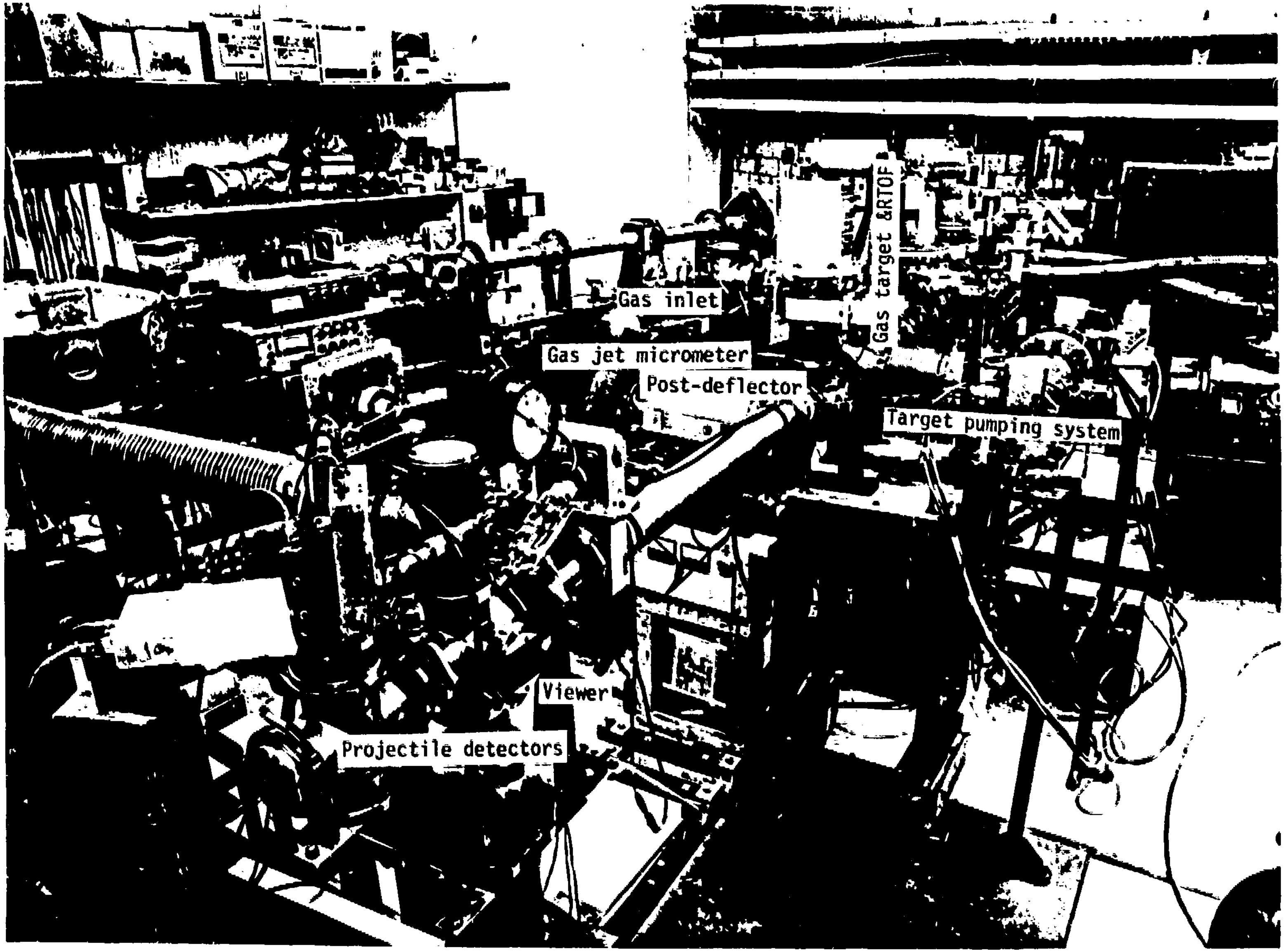

TRANSPARENCY NO. 7

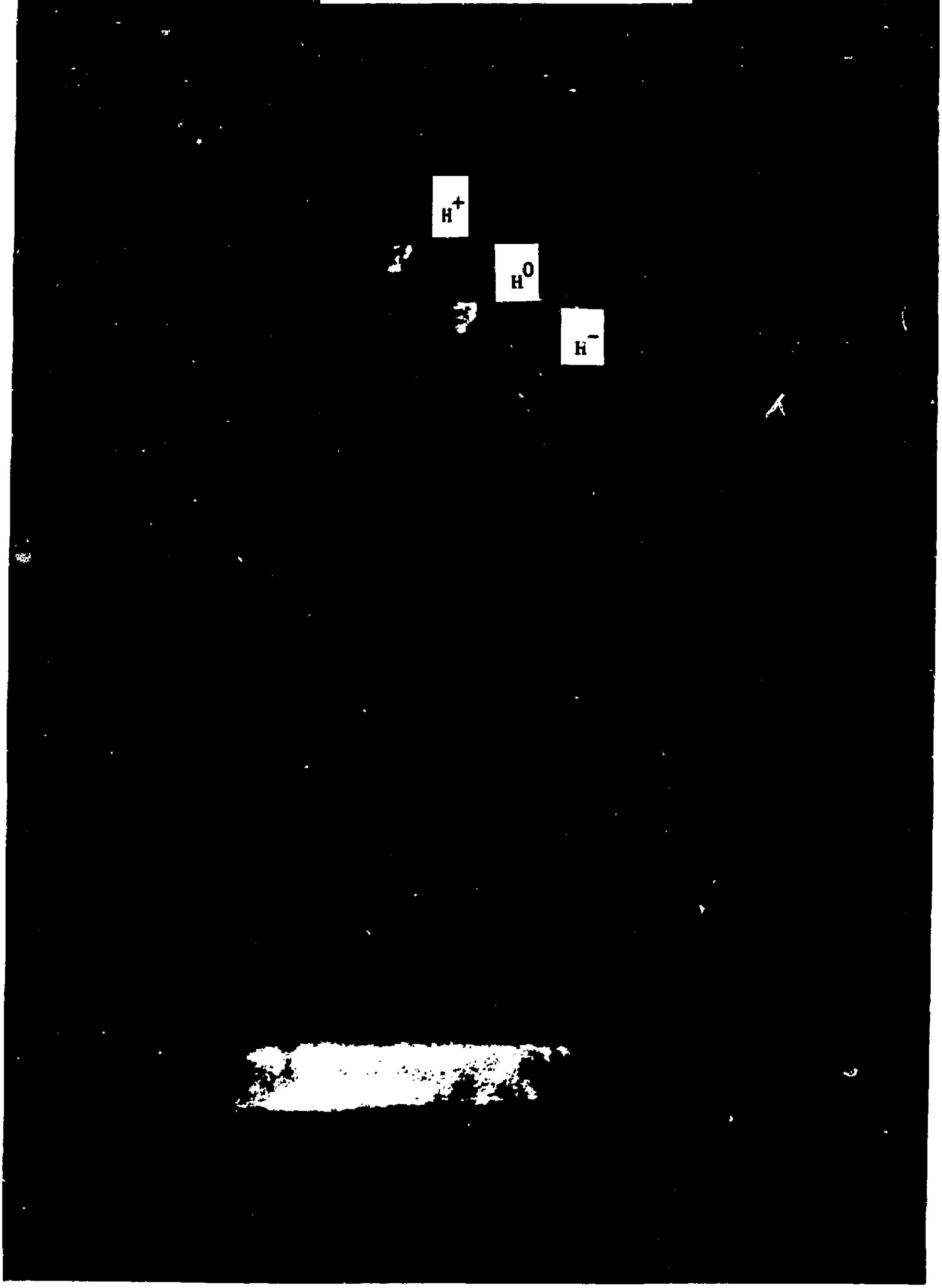

TRANSPARENCY NO. 8

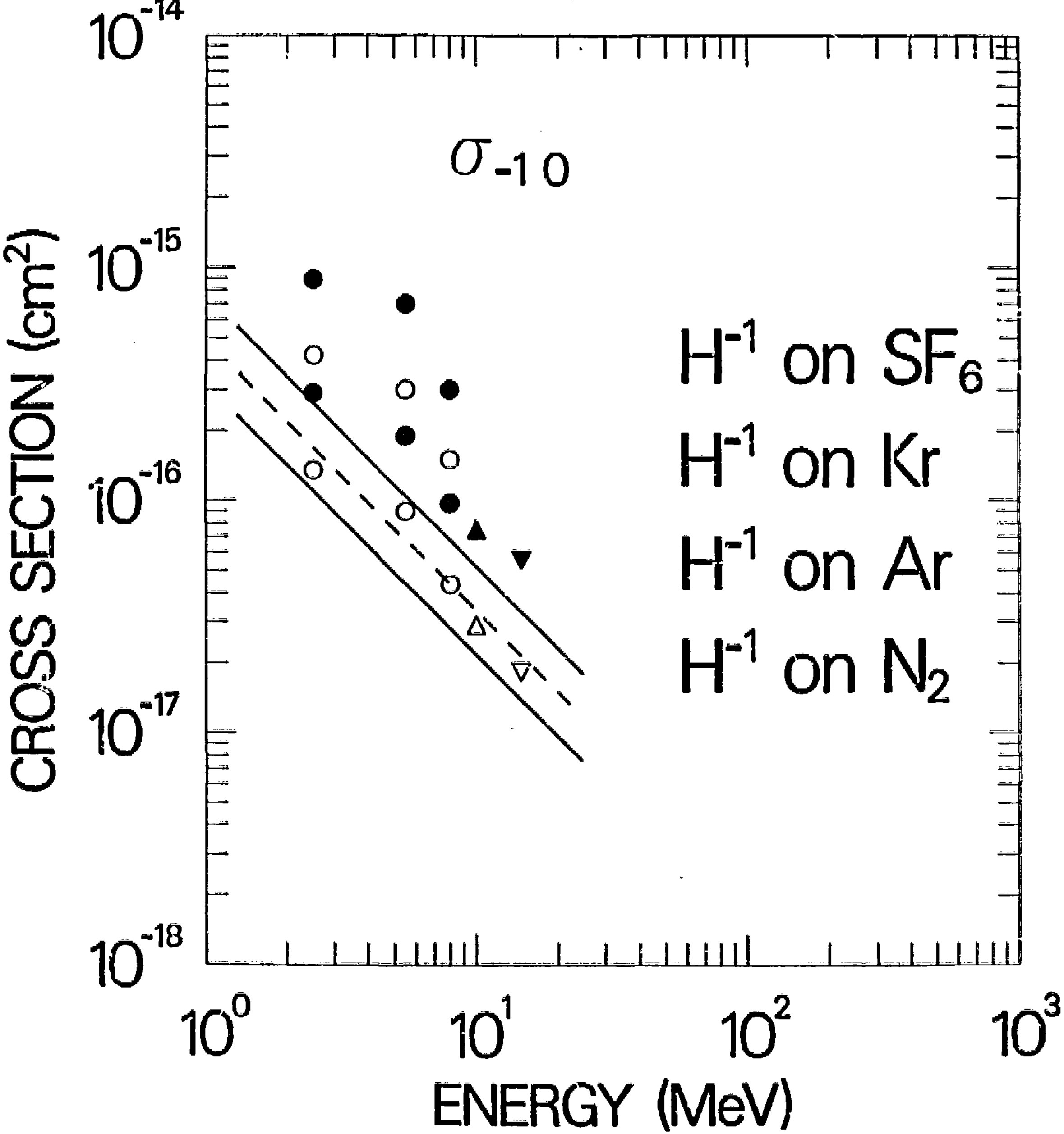

TRANSPARENCY NO. 9

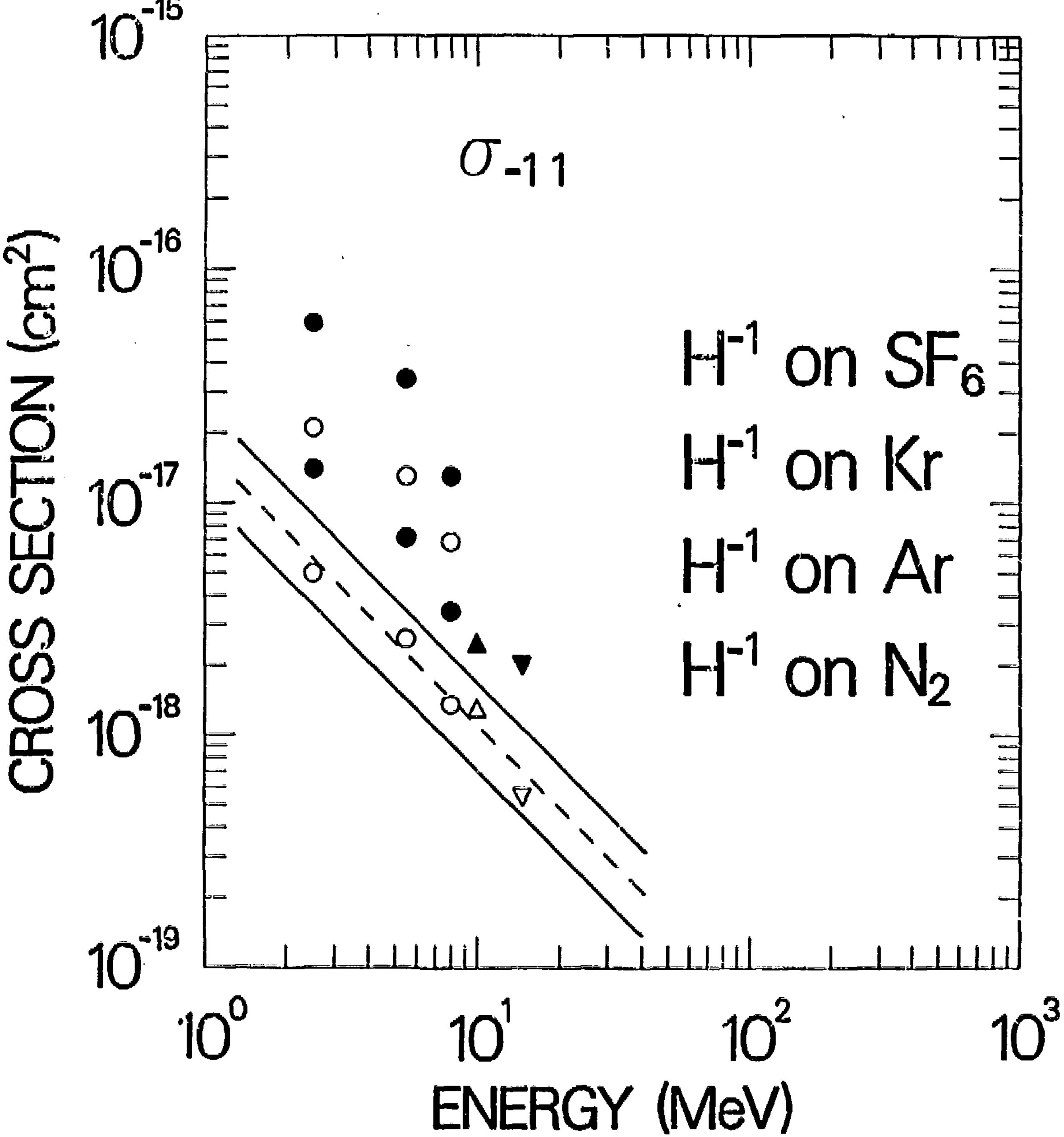

TRANSPARENCY NO. 10

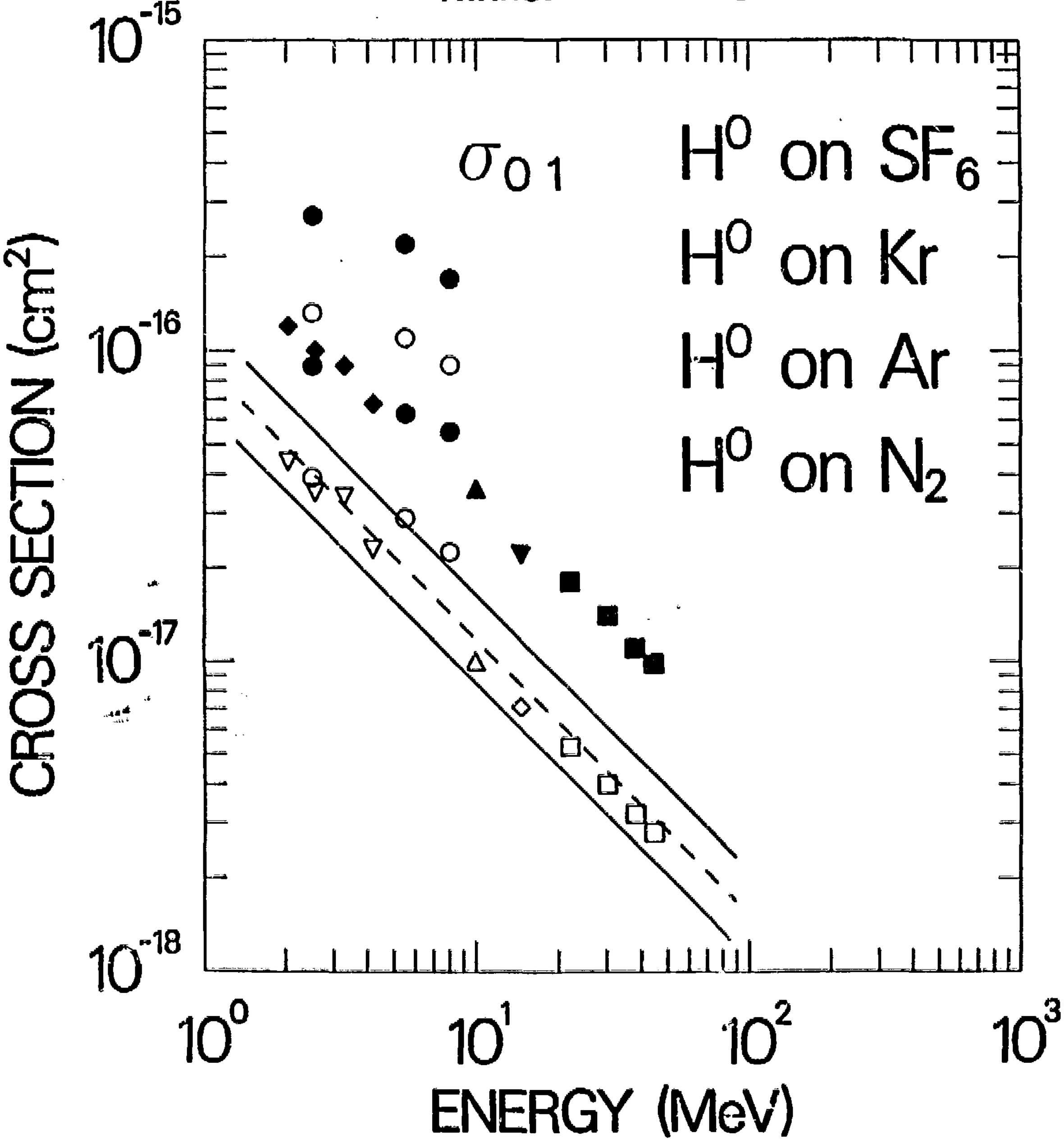

TRANSPARENCY NO. 11